THE JOURNAL OF PHYSICAL CHEMISTRY B



Letter

# Plasma Induced Grafting Carboxymethyl Cellulose on Multiwalled Carbon Nanotubes for the Removal of UO from Aqueous Solution

Dadong Shao, Zhongqing Jiang, Xiangke Wang, Jiaxing Li, and Yuedong Meng

*J. Phys. Chem. B*, **2009**, 113 (4), 860-864 • DOI: 10.1021/jp8091094 • Publication Date (Web): 07 January 2009



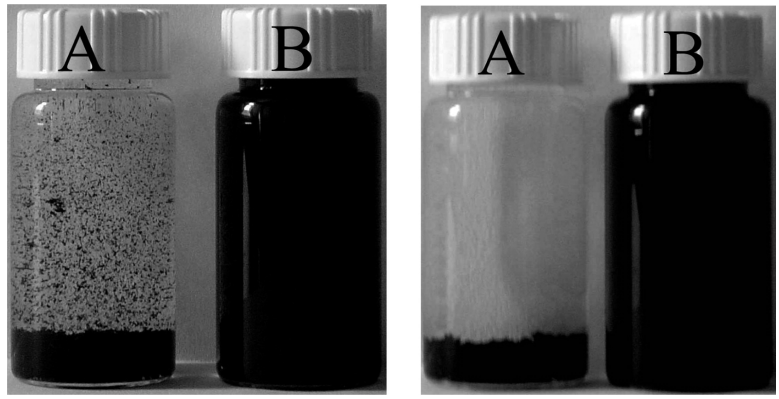


## More About This Article

Additional resources and features associated with this article are available within the HTML version:

- Supporting Information
- Access to high resolution figures
- Links to articles and content related to this article
- Copyright permission to reproduce figures and/or text from this article

View the Full Text HTML



The Journal of Physical Chemistry B is published by the American Chemical Society. 1155 Sixteenth Street N.W., Washington, DC 20036

THE JOURNAL OF PHYSICAL CHEMISTRY B LETTERS

**2009,** *113,* 860–864
Published on Web 01/07/2009

# Plasma Induced Grafting Carboxymethyl Cellulose on Multiwalled Carbon Nanotubes for the Removal of $UO_2^{2+}$ from Aqueous Solution

**Dadong Shao, Zhongqing Jiang, Xiangke Wang,* Jiaxing Li, and Yuedong Meng**

*Key Laboratory of Novel Thin Film Solar Cells, Institute of Plasma Physics, Chinese Academy of Sciences, P.O. Box 1126, 230031, Hefei, P.R. China*

*Received: October 15, 2008; Revised Manuscript Received: December 23, 2008*

Carboxymethyl cellulose (CMC) is grafted on multiwalled carbon nanotubes (MWCNT) by using plasma techniques. The CMC grafted MWCNT (MWCNT-*g*-CMC) is characterized by using Fourier transform infrared spectra (FT-IR), Raman spectra, powder X-ray diffraction (XRD), thermogravimetric analysis (TGA)−differential thermal analysis (DTA), scanning electron microscopy (SEM), and $N_2$-BET methods in detail. The application of MWCNT-*g*-CMC in the removal of $UO_2^{2+}$ from aqueous solution is investigated. MWCNT-*g*-CMC has much higher sorption ability in the removal of $UO_2^{2+}$ than raw MWCNT. The MWCNT-*g*-CMC is a suitable material in the preconcentration and solidification of heavy metal ions from large volume of aqueous solutions.

## Introduction

Carbon nanotubes (CNTs) have attracted great interest in multidisciplinary study since their discovery by Iijima in 1991.[1] CNTs are relatively new adsorbents that have been proven to possess high adsorption capacity to adsorb many kinds of organic and inorganic pollutants,[2] which suggests that CNTs are suitable material to remove pollutants if they can be produced in large scale and at low price. However, the inherent insolubility in most organic and aqueous solvents, poor chemical and biological compatibility of CNTs are the major limitations to the solution phase manipulation, which greatly hinders the application of CNTs in real work.[3] Therefore, research on CNTs has recently been extended to include the modifications of surface properties to enhance the compatibility and dispersion property of CNTs. Most modification methods were mainly focused on conventional chemical methods.[3,4] In these methods, large amounts of chemicals were used, which caused environmental pollution. To avoid the use of toxic solvents and/or extreme conditions in most chemical methods, some new methods, such as microwave method[5] and plasma method,[6] were applied to modify CNTs recently.

Plasma induced grafting treatment is a promising method to introduce functional groups to a material surface without altering the material bulk properties.[7] Plasma grafting functional groups to substance surfaces can enhance the chemical functionality.[8] However, to the best of our knowledge, the research works on plasma induced grafting functional groups on CNTs to improve the adsorption capacity and the dispersion property of CNTs and the application of grafted CNTs in the removal of pollutants from aqueous solutions are not available.

As natural polysaccharide and the most abundant renewable organic material, celluloses can adsorb metal ions due to the chelation of metal ions with carbonyl oxygen and formation ionic bonds with acidic groups of cellulose.[9] Modification of cellulose by grafting copolymerization provides a significant method to alter the physical and chemical properties.[10] Carboxymethyl cellulose (CMC) is one important cellulose derivative with very good water solubility.[11] Thereby, the graft of CMC to CNTs can improve the dispersion of CNTs and enhances the adsorption capacity of CNTs to adsorb metal ions because of the strong complexation ability of CMC with metal ions.

Herein, we first synthesized the multiwalled carbon nanotubes (MWCNT) grafted with CMC (denoted as MWCNT-*g*-CMC) by plasma induced grafting method, and used MWCNT-*g*-CMC to remove $UO_2^{2+}$ from aqueous solution by batch technique.

## Experimental Methods and Results

**Plasma Induced Graft Procedure.** Raw MWCNT was treated by $N_2$ plasma in a custom-built grafting reactor for 40 min under continuous stirring. The plasma treatment conditions were $N_2$ plasma (10 Pa), 70 W, 650 V, and 60 mA. Thus plasma treated MWCNT was denoted as MWCNT-treat.

CMC solution (100 mL 1.50 g/L) was injected into the grafting reactor after MWCNT-treat in the grafting reactor was heated to 80 °C after plasma induced treatment process. Then MWCNT grafted with CMC was stirred at 80 °C for 1 week under continuous stirring. The derived sample was repeatedly washed with Milli-Q water until no CMC was detected by using high performance liquid chromatography−mass spectrometry (HPLC−MS) methods in the supernatant. Each time, the MWCNT-*g*-CMC sample was separated from the suspension by centrifugation at 18 000 rpm for 60 min (BECKMAN COULTER 64R). At last, the sample was dried in oven at 95 °C for 24 h, and thus MWCNT-*g*-CMC material was obtained.

**Characterization.** MWCNT-*g*-CMC was characterized by Fourier transform infrared spectra (FT-IR), Raman spectra, powder X-ray diffraction (XRD), thermogravimetric analysis (TGA)−differential thermal analysis (DTA), scanning electron microscopy (SEM), and $N_2$-BET methods. Detailed illustrations are listed in Support Information SI-3.

* Corresponding author. E-mail: xkwang@ipp.ac.cn.

10.1021/jp8091094 CCC: $40.75 

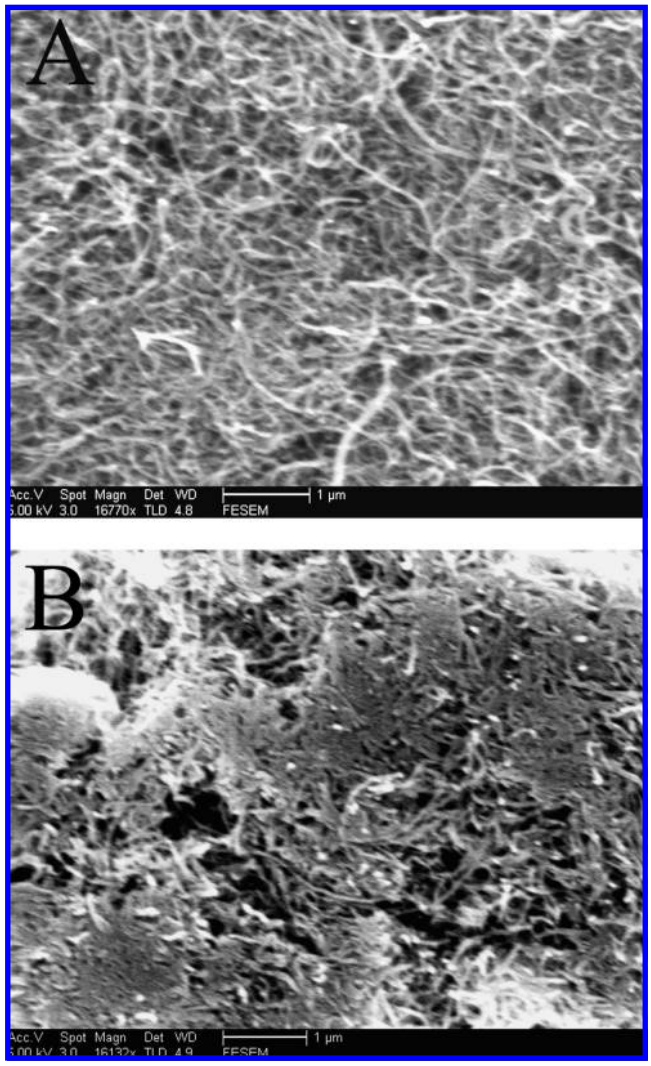


**Figure 1.** SEM images of raw MWCNT (A) and MWCNT-*g*-CMC (B).

The microstructure transformation of raw MWCNT and MWCNT-*g*-CMC are observed by SEM. As can be seen from Figure 1, raw MWCNT and MWCNT-*g*-CMC are curled and entangled, but their stacking morphology is different. MWCNT-*g*-CMC (Figure 1B) has a more compact stacking morphology compared with raw MWCNT (Figure 1A). This is due to the strong interaction between the oxygen-containing functional groups of CMC on the external walls of MWCNT. The polystyrene and diamine modified MWCNT by chemical methods showed very similar SEM images to MWCNT-*g*-CMC.[12]

The microstructure transformation of MWCNT and MWCNT-*g*-CMC can also influence others properties, such as specific surface areas (see Supporting Information Figure SI-1).

As can be seen from the FT-IR spectrum of CMC in Figure 2A, CMC has characteristic bands of −OH at 3420 and 1330 $cm^{-1}$, C−H at 2920 and 2850 $cm^{-1}$, $COO^-$ at 1610 and 1420 $cm^{-1}$, and CH−O−$CH_2$ at 1040 $cm^{-1}$. Raw MWCNT has characteristic bands of graphite structure of MWCNT at 1610 $cm^{-1}$, disordered structure of MWCNT at 1390 $cm^{-1}$, −OH at 3420 $cm^{-1}$, C−H at 2920 and 2850 $cm^{-1}$, $COO^-$ at 1730 and 1450 $cm^{-1}$, CH−O−$CH_2$ at 1040 $cm^{-1}$. Comparing with raw MWCNT, MWCNT-treat has a characteristic band at 3720 $cm^{-1}$, which can be due to the −$NH_2$ formed in plasma treatment process. In the FT-IR spectrum of MWCNT-*g*-CMC,

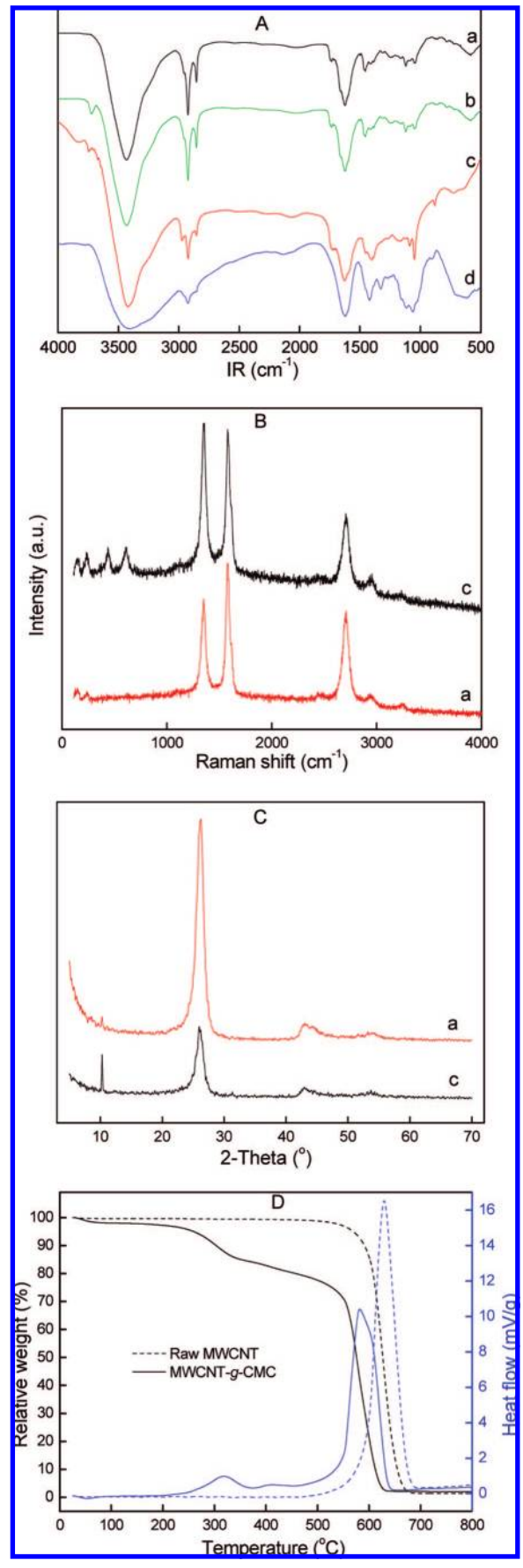


**Figure 2.** FT-IR spectra (A), Raman spectra (B), XRD patterns (C), and TGA-DTA (D) curves of raw MWCNT (a), MWCNT-treat (b), MWCNT-*g*-CMC (c), and CMC (d).

the characteristic band at 880 $cm^{-1}$ is assigned to the hemiacetal,[13] which is formed in plasma induced grafting process. The peak at 3720 $cm^{-1}$ is assigned to $-NH_2$ (testified by MWCNT-treat).[8b,14] The peak at 3420 is assigned to the stretching vibration of $-OH$. The peaks at 1730, 1450 and 1420 $cm^{-1}$ are assigned to the stretching vibrations of carboxylic and carboxylate groups, respectively. The peak between 2920 and 2850 $cm^{-1}$ is assigned to C−H stretching vibration. The peak at 1040 $cm^{-1}$ is due to $CH-O-CH_2$ stretching vibration of CMC (skeletal vibration). Comparing with the peak at 1610 $cm^{-1}$ (assigned to the graphite structure of MWCNT and carboxylate groups of CMC), the peak at 1390 $cm^{-1}$ (assigned to the disordered structure of MWCNT) is enhanced.

The Raman spectra of the raw MWCNT and MWCNT-*g*-CMC are shown in Figure 2B. Comparing with raw MWCNT, two new peaks at 439 and 610 $cm^{-1}$ are related to CMC in the Raman spectrum of MWCNT-*g*-CMC.[15] The Raman and FT-IR spectra both certify that CMC is grafted on MWCNT successfully. The dominant peak is observed at 1352 $cm^{-1}$ for the disordered structure of MWCNT (D mode) and 1580 $cm^{-1}$ for the graphite structure of MWCNT (G mode).[3a,16] The $I_G/I_D$ ratios are 1.39 for raw MWCNT and 0.96 for MWCNT-*g*-CMC. Associating FT-IR with Raman spectra of MWCNT-*g*-CMC, it reveals that the disorder degree of MWCNT-*g*-CMC increases after MWCNT grafted with CMC.

Figure 2C presents the XRD patterns of raw MWCNT and MWCNT-*g*-CMC. The peaks at $2\theta = 10.3$, 26.2, 43.0, and 53.7° are related to the characteristics of MWCNT observed.[17] An obvious diffraction peak at $2\theta = 26.2°$ indicates the crystalline nature of graphite, which is attributed to the graphitic structure of MWCNT. Comparing with raw MWCNT, the diffraction peak at $2\theta = 10.3°$ (corresponding to the graphite structure of MWCNT) of MWCNT-*g*-CMC is enhanced evidently. Combining the changing in Raman spectra, some changes occurred to the structure of MWCNT during the plasma grafting process with CMC.

The thermal property of MWCNT-*g*-CMC is evaluated by TGA-DTA methods. Figure 2D presents the TGA-DTA curves of raw MWCNT and MWCNT-*g*-CMC. According to the TGA-DTA curves of raw MWCNT, the carbon impurity (such as amorphous carbon) in raw MWCNT used in experiments is negligible, and raw MWCNT decompose at 477.6−682.7 °C (endothermic).

Comparing with raw MWCNT, MWCNT-*g*-CMC is less thermal stable responding for the presence of CMC grafted on the surfaces of MWCNT. MWCNT-*g*-CMC shows the characteristic peaks of CMC. In the TGA-DTA curves of MWCNT-*g*-CMC, the 1.89% weight loss at 27.4−84.7 °C (endothermic) can be due to the loss of absorbed water. The 13.4% weight loss at 129.0−362.3 °C (exothermic) and the 4.69% weight loss at 363.1−461.5 °C (exothermic) correspond to the decomposition of CMC.[17] The 77.5% weight loss at 461.5−642.7 °C (exothermic) corresponds to the combustion of carbon residue of CMC[18] and MWCNT. According to the TGA-DTA curves of MWCNT-*g*-CMC, the weight percent of CMC in MWCNT-*g*-CMC is calculated to be 18.1%.

Comparing with raw MWCNT, MWCNT-*g*-CMC has very good dispersion properties in aqueous solution. The MWCNT-*g*-CMC in Milli-Q water does not form aggregation for a long aging time, whereas the raw MWCNT in Milli-Q water forms aggregation at the bottom in a short period of aging time. After 5 min of aging time, most of MWCNT forms aggregation at the bottom of the bottle (see bottle A in the left part of Figure 3). After 5 months of aging time, all MWCNT forms aggregation at the bottom of bottle (see bottle A in the right part of Figure 3). However, no aggregation forms in MWCNT-*g*-CMC suspension even after 5 months of aging time (see bottle B in the right Figure 3).

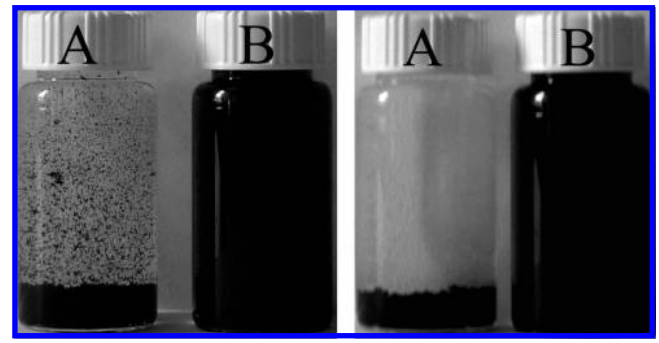


**Figure 3.** Dispersion properties of raw MWCNT (A) and MWCNT-*g*-CMC (B) in Milli-Q water settling for 5 min (left) and 5 months (right).

**Sorption of $UO_2^{2+}$ on Raw MWCNT and MWCNT-*g*-CMC.** Uranium is a representative actinide element. Uranium is very essential element in nuclear and atomic energy program. Moreover, $UO_2^{2+}$ is an important radionuclide both in the environment and in radioactive waste management. To evaluate the sorption property of MWCNT-*g*-CMC, the sorption of $UO_2^{2+}$ from aqueous solution on MWCNT-*g*-CMC and on raw MWCNT was studied. Detailed experimental procedure was described in Support Information SI-6.

The sorption isotherms of $UO_2^{2+}$ on raw MWCNT, on MWCNT-treat, and on MWCNT-*g*-CMC are shown in Figure 4A. The experimental data are simulated by Langmuir model ($C_s = b*C_{s,max}*C_{eq}/(1 + bC_{eq})$), $C_s$ is the concentration of $UO_2^{2+}$ on solid phase, $C_{eq}$ is the concentration of $UO_2^{2+}$ in solution, $C_{s,max}$ is maximum adsorption capacity, and $b$ is the Langmuir constant) very well. The maximum sorption capacity ($C_{s,max}$) of $UO_2^{2+}$ sorption calculated from Langmuir model is $6.0 \times 10^{-5}$ mol/g for raw MWCNT, $1.1 \times 10^{-4}$ mol/g for MWCNT-treat, and $4.7 \times 10^{-4}$ mol/g for MWCNT-*g*-CMC under the experimental conditions. The results indicate that the sorption capacity of MWCNT-*g*-CMC is ∼8 times higher than that of the raw MWCNT in the removal of $UO_2^{2+}$. In MWCNT-*g*-CMC sample, many functional groups such as $-NH_2$ and functional groups of CMC are introduced on the surfaces of MWCNT. These functional groups can form strong complexes with $UO_2^{2+}$ on MWCNT-*g*-CMC surfaces and thereby enhance the sorption capacity of MWCNT-*g*-CMC obviously. Moreover, the plasma treatment can also introduce $-NH_2$ groups on MWCNT surfaces and improves MWCNT-treat sorption capacity in the removal of $UO_2^{2+}$ from aqueous solution.

In the removal of $UO_2^{2+}$ from aqueous solutions, the amount of MWCNT or MWCNT-*g*-CMC used in the process is crucial for the economic application. Under the effective removal percent uncertainties, the less amount of sorbent is used, the lower cost is applied. The effect of sorbent content on the sorption of $UO_2^{2+}$ is shown in Figure 4B. The removal percent of $UO_2^{2+}$ increases with increasing sorbent content. The sorption percent of $UO_2^{2+}$ on MWCNT-*g*-CMC is markedly higher than that of $UO_2^{2+}$ on raw MWCNT and MWCNT-treat. Under the experimental conditions applied, the sorption percent of $UO_2^{2+}$ from solution increases from ∼23% to ∼98% with the increasing MWCNT-*g*-CMC content from 0.10 to 1.0 g/L, whereas the sorption percent of $UO_2^{2+}$ from solution increases only from ∼8% to ∼19% on raw MWCNT and from ∼14% to ∼37% on MWCNT-treat with the increasing sorbent content from 0.10

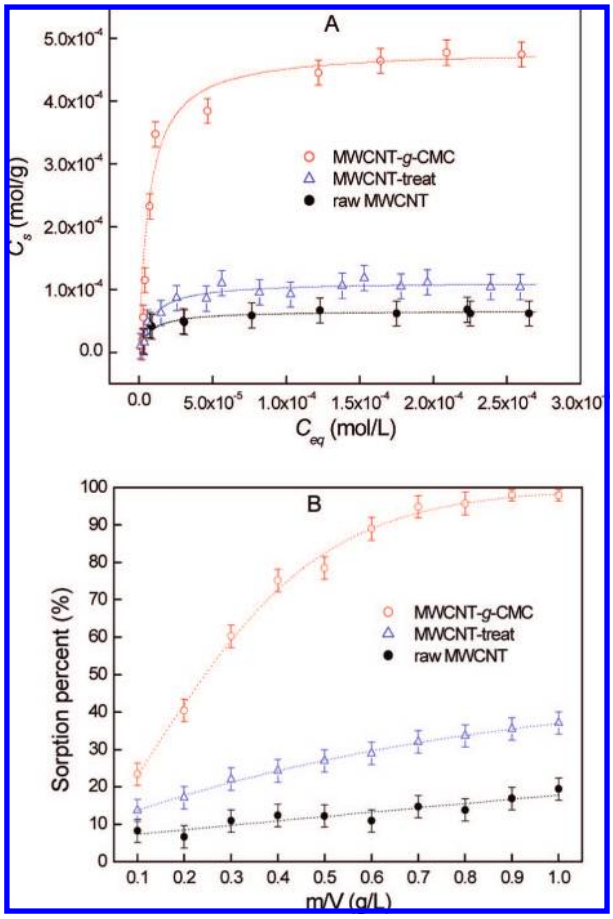


**Figure 4.** Sorption isotherms (A) and effect of sorbent content (B) on the removal of $UO_2^{2+}$ from solution on raw MWCNT, on MWCNT-treat, and on MWCNT-*g*-CMC. $T = 25 \pm 2$ °C, equilibrium time 24 h, pH = $5.0 \pm 0.1$, C[$NaClO_4$] = $1.0 \times 10^{-2}$ mol/L; (A) m/V = 0.4 g/L, (B) $C[UO_2^{2+}]_{(initial)} = 2.00 \times 10^{-4}$ mol/L.

to 1.0 g/L. This is very important for the application of MWCNT-*g*-CMC, MWCNT-treat, or MWCNT in the removal of $UO_2^{2+}$ from solution. If the same amount of MWCNT-*g*-CMC, MWCNT-treat, or MWCNT is used, the removal efficiency of $UO_2^{2+}$ by MWCNT-*g*-CMC is much higher than that of $UO_2^{2+}$ by raw MWCNT and MWCNT-treat.

In the application of MWCNT-*g*-CMC in the removal of $UO_2^{2+}$ from aqueous solutions, the effect of pH value and ionic strength is also crucial because the adsorption of $UO_2^{2+}$ is generally affected by the pH values and ionic strength of the system. The sorption of $UO_2^{2+}$ on MWCNT-*g*-CMC increases with increasing pH in acid solution and decreases with increasing ionic strength at low $NaClO_4$ concentrations (detailed results and discussion are listed in Support Information SI-8 and SI-9).

## Conclusion

CMC can be easily grafted on MWCNT successfully by using plasma technique. The MWCNT-*g*-CMC is easily dispersed in solution and has very high sorption capacity in the removal of $UO_2^{2+}$ from aqueous solution. The MWCNT-*g*-CMC is a very suitable material in $UO_2^{2+}$ pollution cleaning.

**Acknowledgment.** Financial support from National Natural Science Foundation of China (20677058, 20501019) and 973 projects from Ministry of Science and Technology (2007CB936602) are acknowledged. We also express our thanks to Mr. Yicai Shi for helpful technical support.

**Supporting Information Available:** Experimental procedures; characterization methods; proposed grafting mechanism; sorption experiment details; relative proportion of species distribution of U(VI); sorption of U(VI) as a function of pH and ionic strength. This material is available free of charge via the Internet at http://pubs.acs.org.

## References and Notes

(1) Iijima, S. *Nature* **1991**, *354*, 56–58.
(2) (a) Long, Q. R.; Yang, R. T. *J. Am. Chem. Soc.* **2001**, *123*, 2058–2059. (b) Lu, C.; Chiu, H.; Liu, C. *Ind. Eng. Chem. Res.* **2006**, *45*, 2850–2855. (c) Chen, W.; Duan, L.; Zhu, D. *Environ. Sci. Technol.* **2007**, *41*, 8295–8300.
(3) (a) Hong, C.; You, Y.; Pan, C. *Polymer* **2006**, *47*, 4300–4309. (b) Qin, S.; Qin, D.; Ford, W. T.; Resasco, D. E.; Herrera, J. E. *J. Am. Chem. Soc.* **2004**, *126*, 170–176.
(4) (a) Hu, H.; Zhao, B.; Hamon, M. A.; Kamaras, K.; Itkis, M. E.; Haddon, R. C. *J. Am. Chem. Soc.* **2003**, *125*, 14893–14900. (b) Peng, H.; Alemany, L. B.; Margrave, J. M.; Khabashesku, V. N. *J. Am. Chem. Soc.* **2003**, *125*, 15174–15182. (c) Holzinger, M.; Abraham, J.; Whelan, P.; Graupner, R.; Ley, L.; Hennrich, F.; Kappes, M.; Hirsch, A. *J. Am. Chem. Soc.* **2003**, *125*, 8566–8580. (d) Ménard-Moyon, C.; Izard, N.; Doris, E.; Miokowski, C. *J. Am. Chem. Soc.* **2006**, *128*, 6552–6553. (e) Ménard-Moyon, C.; Izard, N.; Doris, E.; Miokowski, C. *J. Am. Chem. Soc.* **2006**, *128*, 14764–14765. (f) Zhang, W.; Swager, T. M. *J. Am. Chem. Soc.* **2007**, *129*, 7714–7715. (g) Islam, M. F.; Rojas, E.; Bergey, D. M.; Johnson, A. T.; Yodh, A. G. *Nano Lett.* **2003**, *2*, 269–273. (h) Yoshida, M.; Koumura, N.; Misawa, Y.; Tamaoki, N.; Matsumoto, H.; Kawanami, H.; Kazaoui, S.; Minami, N. *J. Am. Chem. Soc.* **2007**, *129*, 11039–11041. (i) Pal, A.; Chhikara, B. S.; Govindaraj, A.; Bhattacharya, S.; Rao, C. N. R. *J. Mater. Chem.* **2008**, *18*, 2593–2600. (j) Fukushima, T.; Kosaka, A.; Ishimura, Y.; Yamamoto, T.; Takigawa, T.; Ishii, N.; Aida, T. *Science* **2003**, *300*, 2072–1074.
(5) Brunetti, F. G.; Herrero, M. A.; Muñoz, J. M.; Dı´az-Ortiz, A.; Alfonsi, J.; Meneghetti, M.; Prato, M.; Vázquez, E. *J. Am. Chem. Soc.* **2008**, *130*, 8094–8100.
(6) (a) Chen, Q.; Dai, L.; Gao, M.; Huang, S.; Mau, A. *J. Phys. Chem. B* **2001**, *105*, 618–622. (b) Chen, Q.; Dai, L. *Appl. Phys. Lett.* **2000**, *16*, 2719–2721. (c) Tseng, C. H.; Wang, C. C.; Chen, C. Y. *Chem. Mater.* **2007**, *19*, 308–315. (d) Majumder, M.; Chopra, N.; Hinds, B. J. *J. Am. Chem. Soc.* **2005**, *127*, 9062–9070.
(7) (a) Chevallier, P.; Castonguay, M.; Turgeon, S.; Dubrulle, N.; Mantovani, D.; McBreen, P. H.; Wittmann, J. C.; Laroche, G. *J. Phys. Chem. B* **2001**, *105*, 12490–12497. (b) Olander, B.; Wirsén, A.; Albertsson, A. C. *Biomacromolecules* **2002**, *3*, 505–510.
(8) (a) Lewis, G. T.; Nowling, G. R.; Hicks, R. F.; Cohen, Y. *Langmuir* **2007**, *23*, 10756–10764. (b) Wavhal, D. S.; Fisher, E. R. *Langmuir* **2003**, *19*, 79–85.
(9) Eromosele, I. C.; Bayero, S. S. *Bioresource Technol.* **2000**, *71*, 279–281.
(10) Shen, D.; Huang, Y. *Polymer* **2004**, *45*, 7091–7097.
(11) (a) Biswal, D. R.; Singh, R. P. *Carbohydr. Polym.* **2004**, *57*, 379–387. (b) Vasile, C.; Bumbu, G. G.; Dumitriu, R. P.; Staikos, G. *Eur. Polym. J.* **2004**, *40*, 1209–1215.
(12) (a) Fan, D.; He, J.; Tang, W.; Xu, J.; Yang, Y. *Eur. Polym. J.* **2007**, *43*, 26–34. (b) Meng, H.; Sui, G.; Fang, P.; Yang, R. *Polym.* **2008**, *49*, 610–620.
(13) (a) Vicini, S.; Princi, E.; Luciano, G.; Franceschi, E.; Pedemonte, E.; Oldak, D.; Kaczmarek, H.; Sionkowska, A. *Thermochim. Acta* **2004**, *418*, 123–130. (b) Kim, U. J.; Kuga, S.; Wada, M.; Okano, T.; Kondo, T. *Biomacromolecules* **2000**, *1*, 488–492.
(14) Bhattacharyya, D.; Pillai, K.; Chyan, O. M. R.; Tang, L.; Timmons, R. B. *Chem. Mater.* **2007**, *19*, 2222–2228.
(15) (a) Shen, Q.; Rahiala, H.; Rosenholm, J. B. *J. Colloid Interface Sci.* **1998**, *206*, 558–568. (b) Agarwal, U. P.; Ralph, S. A. *Appl. Spectrosc.* **1997**, *51*, 1648–1655.
(16) (a) Tatsuda, N.; Itahara, H.; Setoyama, N.; Fukushima, Y. *Carbon* **2005**, *43*, 2358–2365. (b) Wu, T.; Lin, Y.; Liao, C. *Carbon* **2005**, *43*, 734–740. (c) Lu, C.; Chiu, H. *Chem. Eng. Sci.* **2006**, *61*, 1138–1145. (d) McGuire, K.; Gothard, N.; Gai, P. L.; Dresselhaus, M. S.; Sumanasekera, G.; Rao, A. M. *Carbon* **2005**, *43*, 219–227. (e) Yi, B.; Rajagopalan, R.; Foley, H. C.; Kim, U. J.; Liu, X.; Eklund, P. C. *J. Am. Chem. Soc.* **2006**, *128*, 11307–11313. (f) Zhou, L.; Ohta, K.; Kuroda, K.; Lei, N.; Matsuishi, K.; Gao, L.; Matsumoto, T.; Nakamura, J. *J. Phys. Chem. B* **2005**, *109*, 4439–4447.
(17) (a) Hsieh, C. T.; Chou, Y. W.; Chen, W. Y. *J. Alloy. Compd.* **2008**, *466*, 233–240. (b) Kumar, V. S.; Kumar, J.; Srivastava, R. K.; Srivastava, A.; Srivastava, O. N. *J. Cryst. Growth* **2008**, *310*, 2260–2263. (c) Chatterjee,

A. K.; Sharon, M.; Banerjee, R.; Neumann-Spallart, M. *Electrochim. Acta* **2003**, *48*, 3439–3446. (d) Iwai, Y.; Hirose, M.; Kano, R.; Kawasaki, S.; Hattori, Y.; Takahashi, K. *J. Phys. Chem. Solids* **2008**, *69*, 1199–1202. (e) Kawasaki, S.; Matsuoka, Y.; Yokomae, T.; Nojima, Y.; Okino, F.; Touhara, H.; Kataura, H. *Carbon* **2005**, *43*, 37–45.

(18) (a) Chauhan, G. S.; Dhiman, S. K.; Guleria, L. K.; Misra, B. N.; Kaur, I. *Radiat. Phys. Chem.* **2000**, *58*, 181–190. (b) Liu, D.; Li, J.; Yang, R.; Mo, L.; Huang, L.; Chen, Q.; Chen, K. *Carbohydr. Polym.* **2008**, *74*, 290–300. (c) Zhang, M. Q.; Rong, M. Z.; Lu, X. *Compos. Sci. Technol.* **2005**, *65*, 2514–2525. (d) Said, H. M.; Alla, S. G. A.; El-Naggar, A. W. M. *React. Funct. Polym.* **2004**, *61*, 397–404.

JP8091094